


A new genus and species of sabretooth, *Oriensmilus liupanensis* (Barbourofelinae, Nimravidae, Carnivora), from the middle Miocene of China suggests barbourofelines are nimravids, not felids

Xiaoming Wang, Stuart C. White & Jian Guan

To cite this article: Xiaoming Wang, Stuart C. White & Jian Guan (2020): A new genus and species of sabretooth, *Oriensmilus liupanensis* (Barbourofelinae, Nimravidae, Carnivora), from the middle Miocene of China suggests barbourofelines are nimravids, not felids, Journal of Systematic Palaeontology, DOI: [10.1080/14772019.2019.1691066](https://doi.org/10.1080/14772019.2019.1691066)

To link to this article: <https://doi.org/10.1080/14772019.2019.1691066>

 View supplementary material 

 Published online: 08 Jan 2020.


 Submit your article to this journal 

 View related articles 

 View Crossmark data 



A new genus and species of sabretooth, *Oriensmilus liupanensis* (Barbourofelinae, Nimravidae, Carnivora), from the middle Miocene of China suggests barbourofelines are nimravids, not felids

Xiaoming Wang^{a,b,*} , Stuart C. White^c and Jian Guan^d

^aDepartment of Vertebrate Paleontology, Natural History Museum of Los Angeles County, 900 Exposition Boulevard, Los Angeles CA 90007, USA; ^bKey Laboratory of Vertebrate Evolution and Human Origins, Institute of Vertebrate Paleontology and Paleoanthropology, Chinese Academy of Sciences, Beijing 100044, PR China; ^cSchool of Dentistry, University of California, Los Angeles, 10833 Le Conte Avenue, Los Angeles, CA 90095, USA; ^dBeijing Natural History Museum, 126 Tian Qiao Nan Street, Dongcheng District, Beijing, 100050, PR China

(Received 26 July 2018; accepted 31 October 2019)

Since the early 2000s, a revival of a felid relationship for barbourofeline sabretooths has become popular due to recent discoveries of fragmentary fossils from Africa. According to this view, barbourofelines trace their common ancestor with felids through shared similarities in dental morphology going back to the early Miocene of Africa and Europe. However, whether or not such an idea is represented in the basicranial morphology, a conservative area of high importance in family-level relationships, is yet to be tested. A nearly complete skull of *Oriensmilus liupanensis* gen. and sp. nov. from the middle Miocene Tongxin Basin of northern China represents the most primitive known barbourofeline with an intact basicranial region, affording an opportunity to re-examine the relationship of felids and nimravines. We also present an update on East Asian records of barbourofelines. The new skull of *Oriensmilus* possesses a suite of characters shared with nimravines, such as the lack of an ossified (entotympanic) bullar floor, absence of an intrabullar septum, lack of a ventral promontorial process of the petrosal, presence of a small rostral entotympanic on the dorsal side of the caudal entotympanic, and a distinct caudal entry of the internal carotid artery and nerve that pierces the caudal entotympanic at the junction of the ossified and unossified caudal entotympanics. The absence of an ossified bullar floor in *O. liupanensis* and its presence in those from the middle Miocene of Sansan, France thus help to bracket the transition of this character, which must have happened in the early part of the middle Miocene. Spatial relationships between bullar construction and the middle ear configuration of the carotid artery in *Oriensmilus* strongly resemble those in nimravines but are distinctly different from felids and other basal feliforms. Despite the attractive notion that early barbourofelines arose from a Miocene ancestor that also gave rise to felids, the basicranial evidence argues against this view.

<http://zoobank.org/urn:lsid:zoobank.org:pub:2DE98DBC-4D02-4E18-9788-0B0D8587E73F>

Keywords: Barbourofelinae; basicranium; phylogeny; Tongxin; Cenozoic; Asia

Introduction

The sabretooth subfamily Barbourofelinae possesses a highly specialized dentition and peculiar basicranium; a unique combination that presents a major challenge to a clear understanding of its relationships with other families of Carnivora. Its cat-like teeth may suggest a close relationship to Felidae, but are difficult to reconcile with a radically different ear region that shares little resemblance to true cats. Since the beginning of the twenty-first century, several European vertebrate palaeontologists have advanced an idea of a felid relationship for the barbourofelines, based on their tracing of dental features to progressively more primitive forms in the

early Miocene of Africa, which seems to converge on a presumed basal felid dental plan (Morales *et al.* 2001; Morlo *et al.* 2004; Morlo 2006; Robles *et al.* 2013). This represents a reincarnation of previous ideas that dominated nineteenth and early twentieth century vertebrate palaeontology but that fell out of favour after basicranial morphology was introduced to the debate, as largely championed by North American vertebrate palaeontologists (e.g. Tedford 1978; Neff 1983; Hunt 1987). However, Morales *et al.* (2001), who were leading proponents of the former school of thought, acknowledged that such a relationship based on dental morphology needs to be bolstered by a better understanding of the cranial morphology of primitive barbourofelines.

*Corresponding author. Email: xwang@nhm.org

In this study, we describe a skull of a barbourofeline, the best preserved of its kind, from the middle Miocene of China, and address this debate with a detailed analysis of its ear region using computed tomographic (CT) scanning and conventional preparations. The new skull belongs to the most primitive member of the barbourofelines to possess a well-preserved basicranium, a key anatomical region whose early differentiation and subsequent conservation has the potential to sort out the basal radiations of many carnivoran families. This excellently preserved basicranium thus offers an opportunity to re-examine the felid–barbourofeline hypothesis beyond dental characteristics.

Materials and methods

Image processing

The base of the skull was scanned in a NewTom 5G cone-beam CT scanner at the School of Dentistry, University of California at Los Angeles, in the Boosted mode and with an image pixel size of 150 μm . The dcm files produced were imported into Fiji (ImageJ v. 2.0.0), where the images were contrast optimized and converted to 8-bit .tif files. The resulting .tif files were imported into Avizo v. 9.2.0 Lite, where the images were re-oriented to align with anatomical planes. The structures of interest were manually segmented into the bulla, petrosal, rostral entotympanic, basioccipital basisphenoid and mastoid bones. The internal carotid artery was drawn freehand to correspond to modern carnivoran anatomy.

Phylogenetic analysis

Characters and states were manipulated in Mesquite v. 3.6 (Maddison & Maddison 2018). Parsimony analysis was performed in TNT v. 1.5 (Goloboff & Catalano 2016).

Institutional abbreviations

AMNH, American Museum of Natural History, New York, NY, USA; **BNHM**, Beijing Natural History Museum, Beijing, China; **F:AM**, Frick Collection, Department of Vertebrate Paleontology, American Museum of Natural History, New York, NY, USA; **IVPP**, Institute of Vertebrate Paleontology and Paleoanthropology, Chinese Academy of Sciences, Beijing, China; **MNHN**, Muséum National d'Histoire naturelle, Paris, France; **SMNS**, Staatliches Museum für Naturkunde Stuttgart, Stuttgart, Germany; **UCMP**, University of California Museum of Paleontology, Berkeley, CA, USA; **UF**, Florida Museum of Natural History at University of Florida, Gainesville, FL, USA;

UNSM, University of Nebraska State Museum, Lincoln, NE, USA.

Systematic palaeontology

Order **Carnivora** Bowdich, 1821

Family **Nimravidae** Cope, 1880

Subfamily **Barbourofelinae** Schultz, Schultz and Martin, 1970

Oriensmilus gen. nov.

Type and only species. *Oriensmilus liupanensis* gen. and sp. nov.

Etymology. ‘*Oriens*’, Latin for rising (of the sun), commonly referring to East Asia; ‘*smilē*’, Greek for carving knife, in allusion to the long canine tooth of barbourofelines.

Diagnosis. *Oriensmilus* differs from *Prosansanosmilus* in its larger size, taller genial flange, taller and larger P4 preparastyle and parastyle, more reduced P4 protocone, smaller p3 with distinct anterior accessory cusp, more recumbent p4, and m1 lacking metaconid and talonid (Morlo *et al.* 2004). It is distinguished from *Albanosmilus* and more advanced barbourofelines in its smaller size, lack of a postorbital bar, less well-developed genial flange, narrower palate, more lingual bulging of P3, less well-differentiated P4 preparastyle, presence of a small P4 protocone, and less reduced p3 (Robles *et al.* 2013). *Oriensmilus liupanensis* has the following (mostly primitive) characteristics that distinguish it from *Sansanosmilus palmidens*, the morphologically closest species, and more derived species of barbourofelines: ventral floor of bulla not ossified; medial wall of bulla not expanded toward the midline (bulla less inflated); alisphenoid canal anterior (not medial) to the foramen ovale; less downwardly expanded occipital condyle; more rounded profile of supraoccipital shield; posterior border of incisive foramen in front of posterior edge of canines; posteriorly tapered pterygoid; less enlarged postorbital process of frontal and postorbital bar absent; broader palate with a more inwardly rotated P3; lingually swelled P3; P3 posterior accessory cusp undivided; presence of a small protocone on P4; and less reduced M1.

Oriensmilus liupanensis sp. nov.

(Figs 2–7, 9; Table 1)

1841 *Sansanosmilus palmidens* (Blainville); Chen & Wu 1976, 7.

2013b *Sansanosmilus* sp. (Qiu *et al.*); Wang *et al.* 2016, 798, fig. 4G.

Table 1. Dental measurements (in mm) of Chinese barbourofelines and those of European and North American species that closely bracket the Chinese forms. Measurements from European materials are mostly derived from the literature (Geraads & Güleç 1997; Morlo *et al.* 2004; Peigné 2012; Robles *et al.* 2013) and those from China and North America are our own measurements. **Abbreviations:** Cl, upper canine length; **Cw**, upper canine width; **P3l**, P3 length; **P3w**, P3 width; **P4l**, P4 length; **P4w**, P4 width; **M1l**, M1 length; **M1w**, M1 width; **cl**, lower canine length; **cw**, lower canine width; **p2l**, p2 length; **p2w**, p2 width; **p3l**, p3 length; **p3w**, p3 width; **p4l**, p4 length; **p4w**, p4 width; **m1l**, m1 length; **m1w**, m1 width. *Indicates an estimate.

Taxon	Site	Specimen	Cl	Cw	P3l	P3w	P4l	P4w	M1l	M1w	cl	cw	p2l	p2w	p3l	p3w	p4l	p4w	m1l	m1w
<i>Prosansosmilus peregrinus</i>	Bezian, France	MHNP 7212				23.8	11.2													
<i>Prosansosmilus peregrinus</i>	Langenau, Germany	SMNS 41482									8.4	6.2	1.2	1.2	9.5	4.4	15.6	6.3	17.0	7.6
<i>Oriensmilus liupanensis</i>	Jiulongkou, Hebei	IVPP V4831			12.6	5.5	29.8	8.0	4.0	11.3										
<i>Oriensmilus liupanensis</i>	Tongxin	AMNH FM 145755			10.5	4.4	27.4	8.0	3.8	9.7	7.0	4.5			7.5	3.3	14.5	5.9	17.5	8.4
<i>Oriensmilus liupanensis</i>	Gunziling, Tongxin	IVPP V25220	18.2	8.1	14.0	5.9	28.8	10.5	4.0	10.4										
<i>Oriensmilus liupanensis</i>	Tairum Nor, Tunggur	IVPP V25221					30.1	8.4												
<i>Sansanosmilus palmidens</i>	Sansan, France	MNHN Sa 451	16.5	7.6	10.7	4.8	25.3	8.6	3.4	8.8										
<i>Sansanosmilus palmidens</i>	Sansan, France	MNHN Sa 468					28.7	8.1												
<i>Sansanosmilus palmidens</i>	Sansan, France	MNHN Sa xxx					28.2	8.7												
<i>Sansanosmilus palmidens</i>	Sansan, France	MNHN Sa 453																		
<i>Sansanosmilus palmidens</i>	Sansan, France	MNHN Sa 454																		
<i>Sansanosmilus palmidens</i>	Sansan, France	MNHN Sa 456									9.5	5.0								
<i>Sansanosmilus palmidens</i>	Sansan, France	MNHN Sa 455																		
<i>Sansanosmilus palmidens</i>	Sansan, France	MNHN Sa 458																		
<i>Sansanosmilus palmidens</i>	Sansan, France	MNHN Sa 459																		
<i>Sansanosmilus palmidens</i>	Sansan, France	MNHN Sa 460																		
<i>Albanosmilus jourdani</i>	Platybelodon	AMNH 26608					37.0	10.5												
<i>Albanosmilus jourdani</i>	Q, Tunggur																			
<i>Albanosmilus jourdani</i>	Tunggur Fm	IVPP V2882					35*	9.4												
<i>Albanosmilus jourdani</i>	La Grive-Saint-Alban																			
<i>Albanosmilus jourdani</i>	San Quirico	Individual 1					37.0	12.0												
<i>Albanosmilus jourdani</i>	San Quirico	Individual 2																		
<i>Albanosmilus jourdani</i>	Los Valles de	LVF-4001			11.0	5.0	34.5	9.0	4.0	5.5										
<i>Albanosmilus jourdani</i>	Fuentiduena																			
<i>Albanosmilus jourdani</i>	Los Valles de	LVF-1172																		
<i>Albanosmilus jourdani</i>	Fuentiduena																			
<i>Albanosmilus jourdani</i>	Los Valles de	LVF-2/77																		
<i>Albanosmilus jourdani</i>	Fuentiduena																			
<i>Albanosmilus jourdani</i>	Los Valles de	LVF-ss 10			9.3	3.7														
<i>Albanosmilus jourdani</i>	Los Valles de	LVF-79							4.2	10.1										
<i>Barbourofelis piveteaui</i>	Fuentiduena																			
<i>Barbourofelis piveteaui</i>	Yaslioren, M	TRQ 1016 & 1017																		
<i>Barbourofelis piveteaui</i>	Sinap Fm																			
<i>Barbourofelis piveteaui</i>	M Sinap Fm, Turkey	06-AKM-0276	17.4	6.0	8.0	4.3	40.3	9.5	3.5	6.5	7.3	5.5								
<i>Barbourofelis whitfordi</i>	Quinn Canyon,	UNSM 25546									10.0	5.5								
<i>Barbourofelis whitfordi</i>	Cap Rock M																			
<i>Barbourofelis whitfordi</i>	Big Spring	UCMP 32307																		
<i>Barbourofelis whitfordi</i>	Canyon, SD																			
<i>Barbourofelis whitfordi</i>	E Clayton Q	F:AM 61858									9.5	6.0	3.1							
<i>Barbourofelis whitfordi</i>	E Clayton Q	F:AM 61857									8.2	6.1								

(Continued)

Table 1. (Continued).

Taxon	Site	Specimen	Cl	Cw	P3l	P3w	P4l	P4w	M1l	M1w	cl	cw	p2l	p2w	p3l	p3w	p4l	p4w	m1l	m1w
<i>Barbourofelis whitfordi</i>	MacAdams Q	F:AM 69455									7.3	5.0			7.5	3.8	17.1	6.9	22.6	9.0
<i>Barbourofelis whitfordi</i>	MacAdams Q	F:AM 69456													7.4	4.0	17.2	6.7	23.0	9.6
<i>Barbourofelis whitfordi</i>	MacAdams Q	F:AM 69453				32.0														
<i>Barbourofelis whitfordi</i>	MacAdams Q	F:AM 69454	17.0	6.3																
<i>Barbourofelis morrissi</i>	Leptarctus Q	F:AM 79999	25.0	9.0		42.1	11.5	4.7	8.4	8.6	6.1			5.8	4.7	17.4	8.3	26.5	10.0	
<i>Barbourofelis morrissi</i>	Leptarctus Q	F:AM 61870	26.0	8.8	10.8	5.3	43.3	11.3											27.0	11.2
<i>Barbourofelis morrissi</i>	Leptarctus Q	F:AM 61869																		
<i>Barbourofelis morrissi</i>	H.H.B.Q.	F:AM 61963																		
<i>Barbourofelis morrissi</i>	Wade Q	F:AM 61850	27.4	9.7	9.4	5.1	45.1	10.8												
<i>Barbourofelis morrissi</i>	Wade Q	F:AM 61980									9.8	5.5			8.7	4.7	17.2	7.5	27.0	11.1
<i>Barbourofelis morrissi</i>	Hans Johnson Q	F:AM 61877									10.2	6.5					18.0	7.9	25.6	10.0
<i>Barbourofelis morrissi</i>	Hans Johnson Q	F:AM 80000													6.1	4.7	17.9	8.2	26.2	9.5
<i>Barbourofelis morrissi</i>	Hans Johnson Q	F:AM 61875	30.4	8.7	8.6	5.1	39.5	11.6												
<i>Barbourofelis morrissi</i>	Hans Johnson Q	F:AM 61878																		
<i>Barbourofelis morrissi</i>	Hans Johnson or Xmas Q	F:AM 25201									10.4	5.8			8.3	4.7	20.0	8.2	26.3	11.2
<i>Barbourofelis morrissi</i>	Machairodus Q	F:AM 61900																		
<i>Barbourofelis morrissi</i>	Machairodus Q	F:AM 61896																		
<i>Barbourofelis morrissi</i>	Machairodus Q	F:AM 61895																		
						9.3	4.8	35.8	11.2											

Holotype. IVPP V25220, nearly complete skull with left and right C, P3-4 and M1 alveoli (Figs 3, 4, 6, 7, 9).

Diagnosis. As for genus.

Etymology. Refers to the Liupan Mountains (Liupan Shan); the Tongxin Basin is located at the northern foothills of the Liupan Mountains.

Type locality and horizon. IVPP V25220 is from Gunziling, about 10–12 km south of the small village Dingjia'ergou (Qiu *et al.* 2013b, p. 59) in the Tongxin Basin, Tongxin County, Ningxia Hui Autonomous Region; upper part of Zhang'enbao Formation (Fig. 1).

Referred specimens. From the Tongxin area: BNHM uncatalogued specimen (AMNH cast FM 145755), the rostral part of a skull with left and right I2–3, dC and erupting permanent C, P3–M1 (left M1 broken), complete left jaw with broken i1–3, c, p3–m1 (Fig. 5) – NB, exact locality information for the BNHM specimen is unknown as it was collected by local farmers and acquired by BNHM teams led by Jian Guan (Guan 1988; Guan & Zhang 1993) and multiple 'Dragon Bone caves' were excavated by farmers and concentrated in the upper strata within the Dingjia'ergou wash (red star in Fig. 1). From Jiulongkou, Cixian, Hebei Province: IVPP V4831, left premaxilla with I2-3, left P3, right P4 and left m1 (Chen & Wu 1976, pl. I, fig. 2), Shanwangian Land Mammal age. From Tairum Nor, Tunggur Formation, Inner Mongolia: IVPP V25221, isolated right P4, from locality 348, collected by Feng Wenqing on 5 August 2003 (Fig. 2F–H).

Fauna, strata and age. Vertebrate fossils, most of them purchased from local farmers in the Tongxin area, became known scientifically in the late 1970s. Preliminary studies of the faunas and strata were attempted (Guan 1988; Guan & Zhang 1993), although poor documentation and contradictory interpretations persist to the present day (Qiu *et al.* 2013b, p. 58). Wang *et al.* (2016) synthesized the biostratigraphy of the fossil-bearing strata. They divided the fossil-producing Zhang'enbao Formation (previously the Hongliugou Formation) into three informal members (lower, middle and upper). The Gunziling area is in the southern part of the local exposures and its strata are represented by the Huangjiashui section adjacent to Gunziling Gou, North Gunziling Gou and South Gunziling Gou (Wang *et al.* 2016, fig. 3). Wang *et al.* (2016, table 3) listed *Sansanosmilus* only in Yehuliquanzi Gou and South Gunziling Gou, both of which belong to the same larger wash, within the middle member of the Zhang'enbao Formation, although the exact nature of the material is not described. Fossils are generally found in sandstones

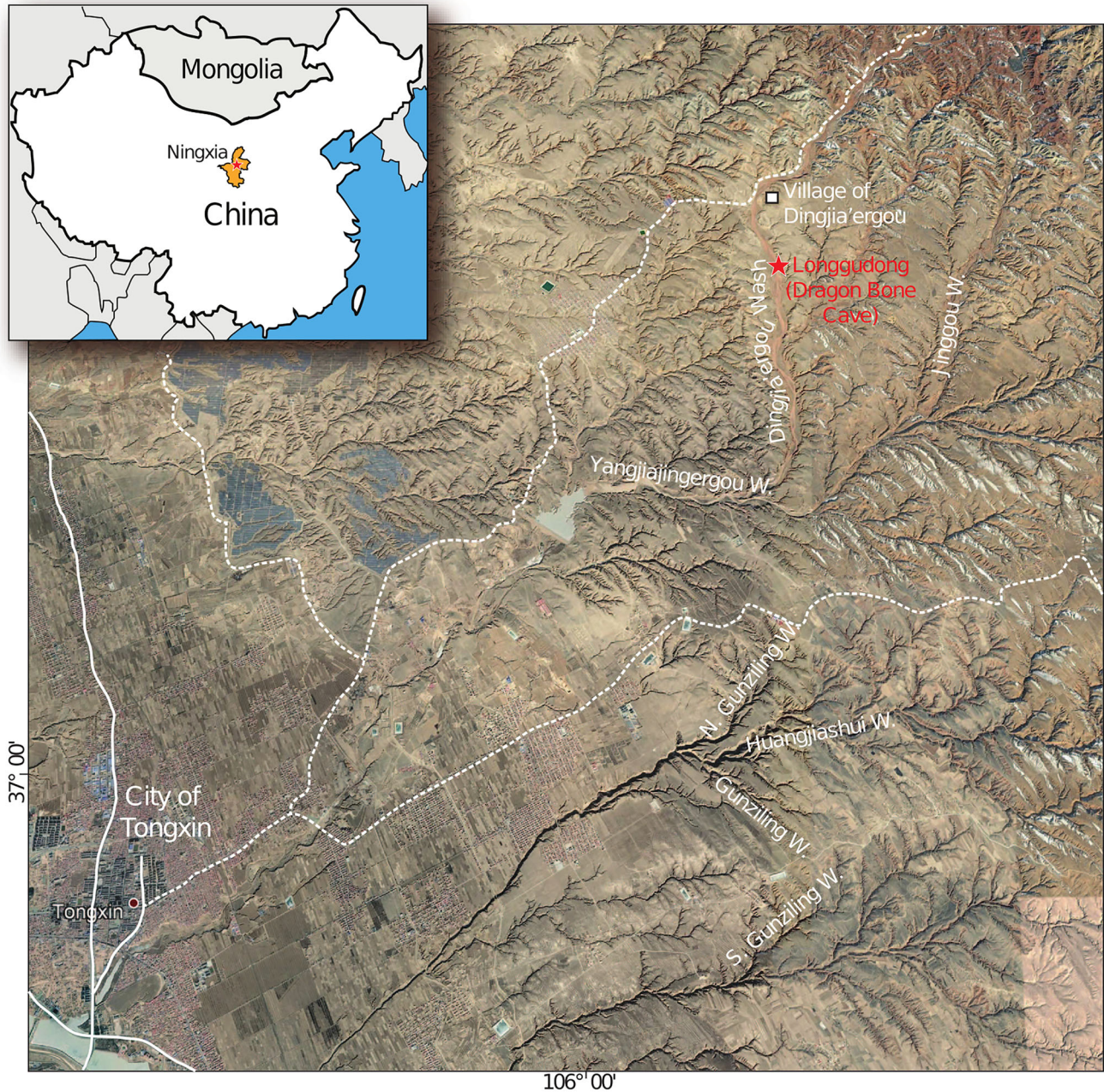


Figure 1. Map of the Tongxin fossil localities in Ningxia Hui Autonomous Region, northern China. Satellite image of Tongxin area ($36^{\circ}57'–37^{\circ}07'N$; $105^{\circ}54'–106^{\circ}02'E$) was downloaded from Google Earth Pro, image date 12 July 2018 (Google Earth Pro v. 7.3.2.5487, 2015). The locality for the BNHM specimen (Dragon Bone Cave) is indicated by a red star. The locality for the IVPP specimen is less certain because there are three named washes that are variations of 'Gunziling' ('North Gunziling', 'Gunziling', and 'South Gunziling'), all of which are potential producers of the specimen (see also Jiangzuo *et al.* 2019, fig. 1).

and IVPP V25220 is presumably from a stratum roughly correlative to the 30 m sandy middle member of the Zhang'enbao Formation. The fossil assemblage from this middle member was named the Ma'erzhuizi Gou Fauna (Wang *et al.* 2016), and these authors also included it within the Dingjia'ergou Fauna.

Thus far, the Dingjia'ergou Fauna (including more than 20 localities spanning more than 200 m of strata) consists of 24 mammals (Qiu *et al.* 2013b, pp. 58, 85), including a pliopithecine primate *Pliopithecus zhanxiangi* (Qiu & Guan 1986; Guan 1988; Harrison *et al.* 1991), a percrocotine hyaenid *Tongxinictis primordialis*

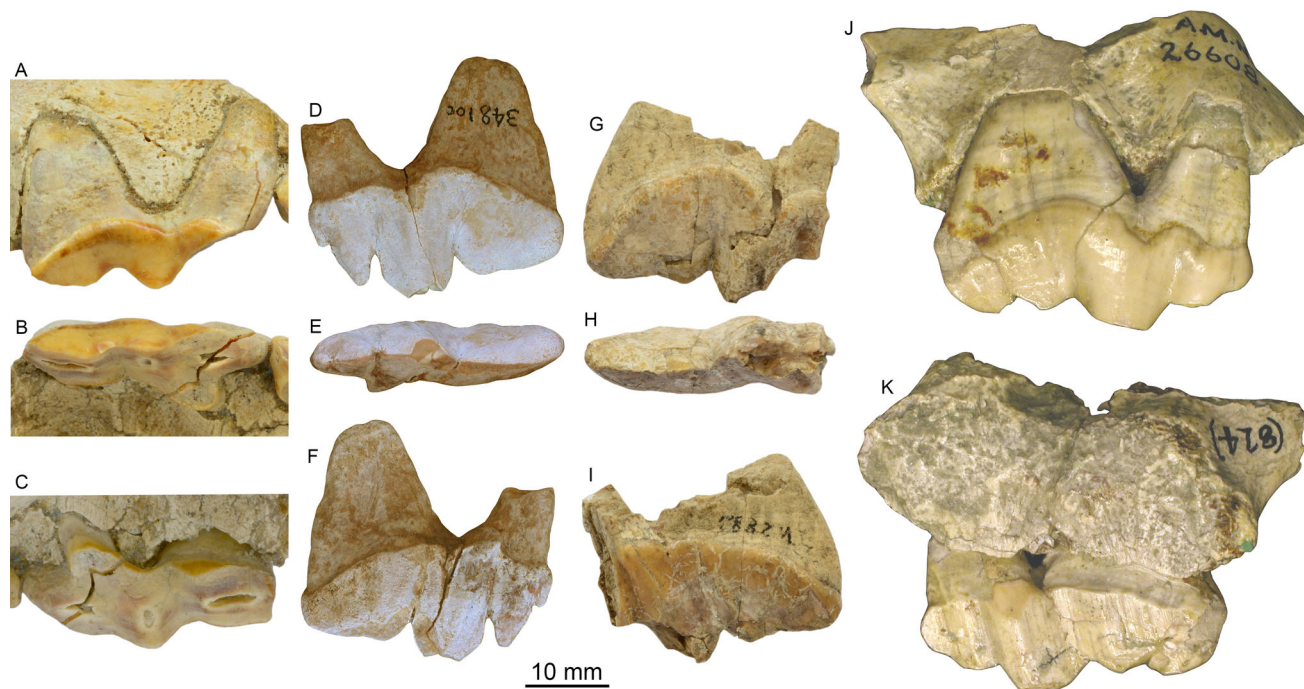


Figure 2. Upper carnassials (P4s) of several Chinese barboourofelines. **A**, buccal, **B**, occlusal and **C**, lingual views of the right P4 of *Oriensmilus liupanensis* (IVPP V25220, holotype) from Gunziling, Tongxin County; **D**, buccal, **E**, occlusal and **F**, lingual views of the left P4 of *O. liupanensis* (IVPP V25221) from Roadmark 348 locality, Tairum Nor, lower Tunggur Formation; **G**, buccal, **H**, occlusal and **I**, lingual views of a partial right P4 of *Albanosmilus jourdani* (IVPP V2882) from an unknown locality in the Tunggur Formation; and **J**, buccal and **K**, lingual views of the right P4 of *A. jourdani* (AMNH 26608) from the *Platybelodon* Quarry, upper Tunggur Formation (Colbert 1939; Wang *et al.* 2003).

(Qiu *et al.* 1988b; Werdelin & Solounias 1991), an iranothere rhino *Ningxiatherium longirhinus* (Chen 1977), two elasmothere rhinos *Beliajevina tongxinensis* (Guan 1988; Qiu *et al.* 2013b) and *Hispanotherium matritense* (Deng 2003), two listriodontine pigs *Kubanochoerus gigas* (Qiu *et al.* 1988c; Guan & Van der Made 1993) and *Bunolistriodon intermedius* (Ye *et al.* 1992), a crown-antlered deer *Stephanocemas palmatus* (Chen 1978; Wang *et al.* 2009), and a shovel-tusked proboscidean *Platybelodon danovi* (*P. tongxinensis*) (Chen 1978; Ye *et al.* 1989). Wang *et al.*'s (2016) more restricted Ma'erzhui Gou Fauna is represented by fossils from the middle member of the Zhang'enbao Formation, and they typified this fauna by *Alloptox gobiensis*, *Platybelodon tongxinensis*, *Hispanotherium matritense* and *Turcocerus* sp. The Dingjia'ergou Fauna *sensu lato* has middle Miocene characteristics, but was placed between the Tunggurian and Shanwangian Chinese Land Mammal stages/ages (Qiu *et al.* 2013b). Qiu *et al.* (2013b) considered the Dingjia'ergou Fauna to be from the upper part of the Hongliugou (Zhang'enbao) Formation and closest to the Belamechetskaya Fauna of the Caucasus, and dated the Dingjiaergou Fauna as 15–16 Ma (Qiu *et al.* 2013b, fig 1.4), because the comparable Belamechetskaya Fauna is bracketed between

marine Chokrakian sediments that are correlated with the middle Badenian Stage in the Paratethys, the latter being around 15 Ma in age (Steinger 1999).

Description

IVPP V25220 is a full adult with well-worn cheek teeth, whereas AMNH FM 145755 represents a young adult with co-occurrence of deciduous and permanent upper canines and no wear on cheek teeth. We therefore describe these two specimens separately in order to provide a sense of ontogenetic variation.

Skull of IVPP V25220

IVPP V25220 (Figs 3, 4) is slightly dorsoventrally crushed and somewhat sheared, with the dorsal portion shifting toward the left-hand side and the ventral portion toward the right. The overall distortion is not too great to visually restore its original proportions. In dorsal views, both nasals are missing; however, the anterior borders of the frontals seem relatively intact, i.e. the nasal–frontal suture is largely preserved. Based on this suture, the posterior border of the nasal forms a



Figure 3. Skull of *Oriensmilus liupanensis* (IVPP V25220, holotype) from Gunziling, Tongxin County in **A**, right lateral; and **B**, dorsal views.

transversely straight line slightly posterior to the anterior border of the infraorbital foramen, similar to the condition seen in an illustrated specimen of *Sansanosmilus palmidens* from Sansan, France (Ginsburg 1961, pl.

XV). The frontal bones above the orbits are broad and form a slightly concave forehead due to a slightly raised postorbital process. The postorbital processes are slender, short and triangular in cross-section. The tips of the

processes are both preserved and extend laterally by about 12 mm from the base of the orbit. The gaps between the postorbital processes of the frontals and the postorbital processes of the jugals are 23 mm on the right side and 16 mm on the left side, the difference due to the leftward shearing of the top of the skull. The temporal crest originating from the tip of the postorbital process is largely transverse for much of its course, with a slight anterior bend, and the left and right crests meet in the middle in front of the postorbital constriction. The sagittal crest is mostly broken at the base but judging from the height of the supraoccipital shield the sagittal crest may be as high as 15 mm at its highest point near the back of the cranium. The supraoccipital shield is fan-shaped in posterior view and is slightly constricted at the level of occipital condyle.

In lateral aspect, the dorsal profile of the skull is slightly concave above the orbit, and the profile of the sagittal crest cannot be accurately observed due to

breakage. The orbital region is too fragmentary to judge the relationships of individual bones. The infraorbital canal has an oval cross-section of 8×6 mm in maximum and minimum dimensions. The long axis of the oval is essentially horizontal, although a certain amount of this is due to a slight dorsoventral compression. The right zygomatic arch is nearly completely preserved. The maximum anterior depth of the arch is 21 mm (22 mm on the left side). The masseter fossa above the posterior root of the P4 is not deeply excavated. The postorbital process of the jugal is small and blunt, and is barely visible in lateral view.

In ventral aspect, the palate is broad, particularly near the area of the carnassial teeth. This broadening of the palate also causes the pterygoid wings to form a large angle, instead of being parallel to each other. The palatine foramen is at the level of the anterior edge of the P3. Individual bones of the palate are not easily discernible due to the advanced stage of fusion.

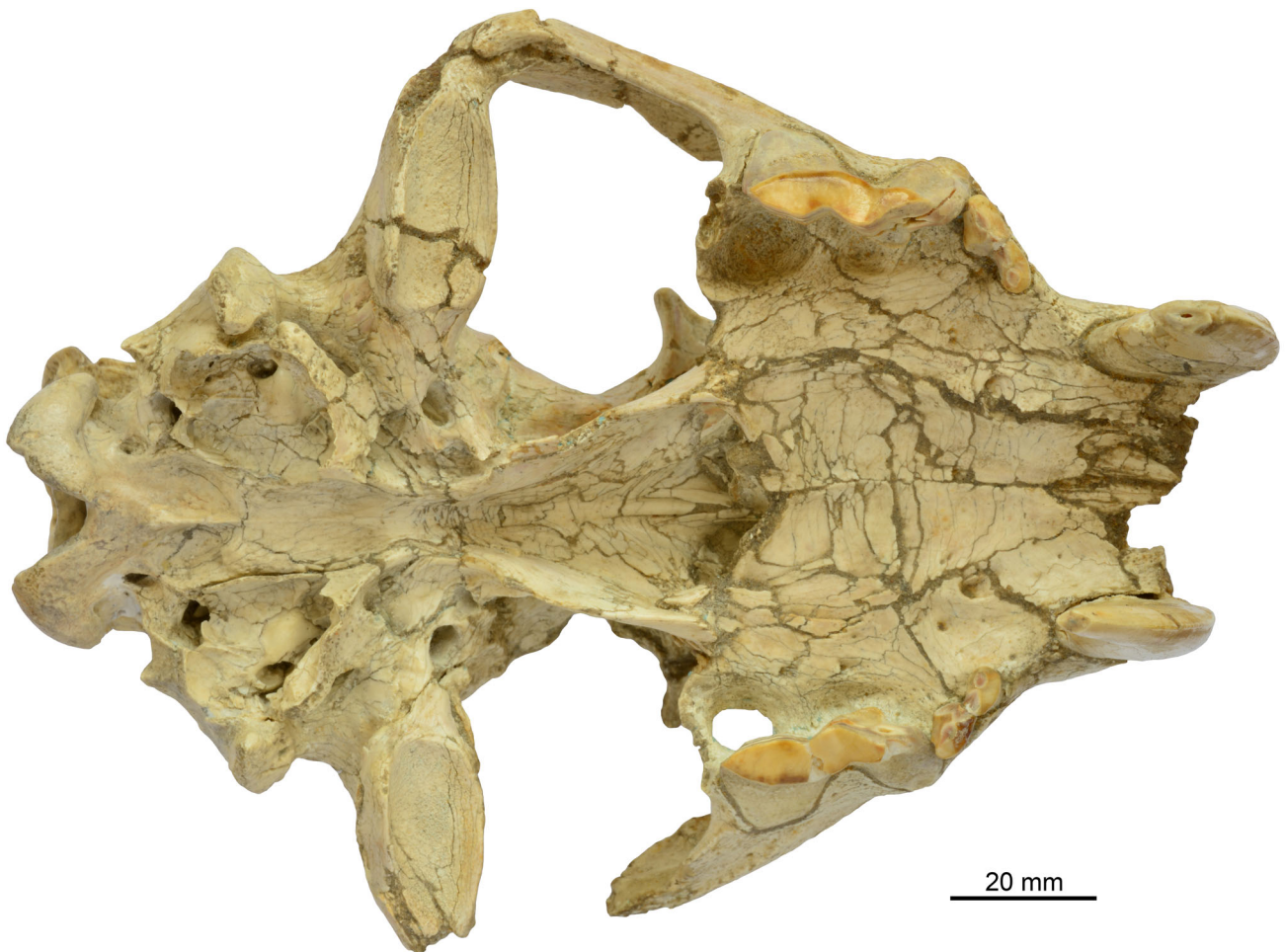


Figure 4. Skull of *Oriensmilus liupanensis* (IVPP V25220) from Gunziling, Tongxin County, in ventral view.

Teeth of IVPP V25220

Much of the premaxilla is missing, as are all upper incisors. The upper canines are well preserved, especially that on the left side. The anterior wall of the left alveolus is missing, exposing the entire length of the root. The distance between the root tip to enamel apex (a small part of the tip is missing) of the left canine is 97 mm, whereas its outer curvature length is ~ 125 mm. The cross-section of the upper canines is proximodistally flattened with an aspect ratio (cross sectional length/width at the maxillary base) of 2.25. A thin lingual and labial blade runs along the entire enamel surface. The labial blade turns slightly proximally, terminating at the anteroproximal corner of the tooth. The lingual blade stays at the centre of the tooth throughout. Extremely fine serrations can be seen along the entire labial and lingual blades.

A diastema of 9.5 mm (left) and 12.4 mm (right) is present between the P3s and upper canines. The anterior edges of the P3s are rotated toward the lingual side to accommodate the broadening of the palate. Both P3s are heavily worn, but individual cusps are still visible, including a large main cusp flanked by an anterior accessory cusp and a posterior accessory cusp, the latter being slightly larger than the former. A distinct lingual bulge is located behind the main cusp of the P3s. The corresponding root below this bulge is also swollen toward the lingual side but there is no discrete rootlet. There is no cingulum on the P3s. A distinct notch on the posterior accessory cusp is lacking, whereas the latter is clearly seen in *Sansanosmilus palmidens* (Ginsburg 1961, pl. XIII) and helps to delineate a small cusp at the distal end.

The upper carnassials (P4s) have suffered from even more wear and lingual tilting, to the point that the pulp cavities for the metacone, paracone and parastyle are all visible (Fig. 2B, C). A white ring lines the pulp cavities is presumably the result of secondary dentine build-up, although radiologically these white linings are not distinguishable in the CT scans. A distinct protocone bulge is located on the lingual side, between the paracone and parastyle. The protocone itself has been worn down to its base but its root is distinct. Wear to the parastyle-preparastyle area is so severe that the individual cusp pattern is no longer visible.

To self-sharpen the carnassial shear, the cutting blades of the P4s are oriented parasagittally and the bodies of the teeth are extensively tilted toward the lingual side, a condition that has been extensively discussed by Bryant and Russell (1995). The roots are completely exposed (dehiscence) on the buccal sides, presumably from resorption of the surrounding maxillary cortical plate. The tips of the roots are slightly bent toward the lingual direction.

Both M1s are lost but their alveoli are preserved with double roots. They are located distally from the distal

edge of P4 and, when present, are not hidden by the P4s in lateral views. The transverse \times anteroposterior alveolar dimensions are 11×5 mm (right) and 10×4 mm (left).

BNHM Tongxin specimen (AMNH FM 145755)

The dorsal surface of the skull is badly damaged – both frontals, left nasal and left maxillary have collapsed around the left orbital area (Fig. 5). The tips of both postorbital processes of the frontal are broken but it is clear that they are far from touching the postorbital processes of jugal to form the postorbital bar seen in advanced barbourofelines: the gap between these two processes is about 22 mm long. The postorbital processes of the frontal are slender and rod-like with a triangular cross-section. The postorbital constriction measures 32 mm transversely, in contrast to 53.7 mm between the tips of the broken postorbital processes. The right zygomatic arch is preserved and has a distinct scar of the masseter muscle along the jugal process. The depth of the zygomatic arch below the orbit is 8 mm. The infraorbital canal is rounded in cross-section and has a diameter of about 7 mm. The palate is short and broad; it measures ~ 55 mm between the posterior border of palatine and posterior alveolar rim of the I1 and has a maximum width of 80.4 mm across the labial margins of the upper carnassials. The incisive foramina are oval with posterior rims aligned with the posterior edge of the upper canines and anterior rims stopping approximately two-thirds of the length of the canines.

Despite the damage suffered by the skull, the lower jaw is almost perfectly preserved, except for the angular process. The horizontal ramus deepens slightly anteriorly, but otherwise maintains a rather gently curved lower border. The maximum depth of the flange is 33 mm and its anterior rim has a sharp lateral edge. The depth of the symphysis is 36.4 mm. The ascending ramus is high; its dorsal tip is at least 9 mm above the apex of the m1 protoconid. The coronoid process is thin and the mandibular fossa is relatively shallow.

AMNH FM 145755 has the tip of its permanent canines still above the lower border of the maxillary and both deciduous canines are still attached, a delayed eruption of upper canines as documented by Bryant (1988) in *Barbourofelis*, *Eusmilus* and *Hoplophoneus*. Much of the anterior surface of the right permanent canine is exposed along the premaxillary–maxillary suture due to damage to the premaxilla. The anterior ridge of the canine is sharp and has fine serrations.

The I2–3 are single-cusped and their tips are hooked slightly posteriorly. Besides a ridge on either side of the incisors there is no accessory cusp. The left deciduous canine measures 13.1×5.2 mm at the base and the undamaged left canine has a maximum length of

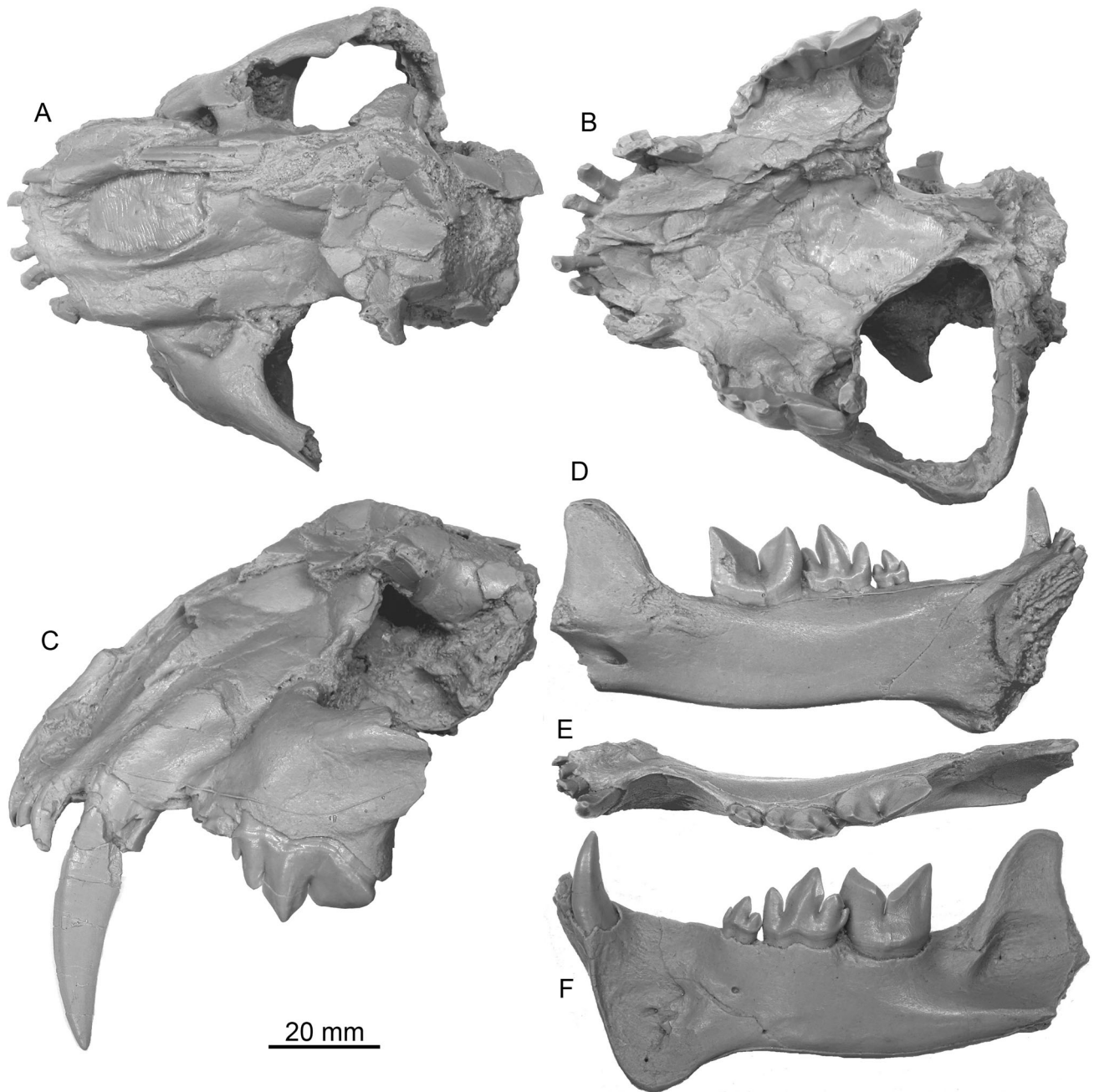


Figure 5. Skull and left jaw of *Oriensmilus liupanensis*, uncatalogued specimen from BNHM (AMNH cast FM 145755), from Tongxin County. **A**, dorsal, **B**, ventral and **C**, lateral views of the skull; **D**, lingual, **E**, occlusal and **F**, buccal views of the left jaw.

44.7 mm from tip to posterior alveolar rim. The upper canines curve posteriorly slightly although they still protrude forward overall. A broad and shallow groove is present on the lingual side of the dC and a very faint indication of a groove is also present on the labial side. There is a short diastema of 8.3 mm (left side) between dC and P3. The right P3 is broken completely and the left P3 still preserves part of the main cusp and much of the posterior accessory cusp (although the tip is broken

off). The P3 is elongate and low-crowned. The P4 shows slight wear on the posterior blade of the paracone and the metastyle, but the anterior blade of the paracone and parastyle and the preparastyle are essentially pristine. The preparastyle is small and its tip is approximately halfway along the anterior edge of the parastyle. A shallow notch, approximately 1.5 mm in depth, separates the preparastyle and parastyle. The parastyle is the same height as the metastyle blade. The notch between

the parastyle and paracone is deep, as is the notch between paracone and metastyle. Extremely fine serrations are present on the unworn blades of the P4. A highly reduced protocone is present toward the lingual side of the paracone: it is not conical and is no more than a rounded ridge protruding from the straight lingual surface of the tooth. The protocone root is closely appressed to the two main roots of the tooth. The enamel–dentine juncture at the protocone is also marked by a dorsal protrusion toward its root. The M1 seems to be double-rooted. Its crown surface is mostly broken on the right side and completely missing on the left side. The outline of the tooth is transversely elongated.

The lower canine curves slightly posteriorly. It has a sharp posterior ridge, which is finely serrated. There is also a prominent lingual ridge from the base to nearly the tip of the tooth. A long diastema of 20 mm spans between the lower canine and p3. The cheek teeth are moderately splayed laterally, corresponding to the broadening of the upper palate. The p3 is double-rooted. It has a main cusp, a small anterior accessory cusp and a larger posterior accessory cusp. A large anterior accessory cusp on the p4 is vertically oriented and separated from the main cusp by a deep notch that reaches to its base. The p4 main cusp has the same height as the m1 paraconid and its main axis

is slightly recumbent. The posterior accessory cusp is about the same height as the anterior one but is slightly stronger. The notch separating the posterior accessory cusp and main cusp is, however, shallower than that of the anterior one. A small but distinct posterior cingular cusp is present on the p4. Both of the premolars have fine serrations along all of their blades. The m1 is formed by the paraconid and protoconid blades separated by a deep carnassial notch that reaches halfway toward the middle of the tooth. The paraconid and metaconid blades suffered from minor wear and, at this early stage of wear, no sign of lateral bending is detectable (but seen in full adults). No metaconid or talonid are visible.

Basicranium of IVPP V25220

The glenoid fossa is slightly lowered, with its dorsal surface for the articulating fossa at the level of the centre of the auditory meatus (Figs 6, 7, 9). The mastoid process is large and inflated. A prominent lateral ridge runs vertically from the ventral tip to the top of the process. The ventral tip is pointed and at the same level as the ventral tip of the glenoid process. The paroccipital process is very small and pointed posteriorly, with its tip hooking slightly ventrally. The process does not cup the posterior aspect of the bulla.

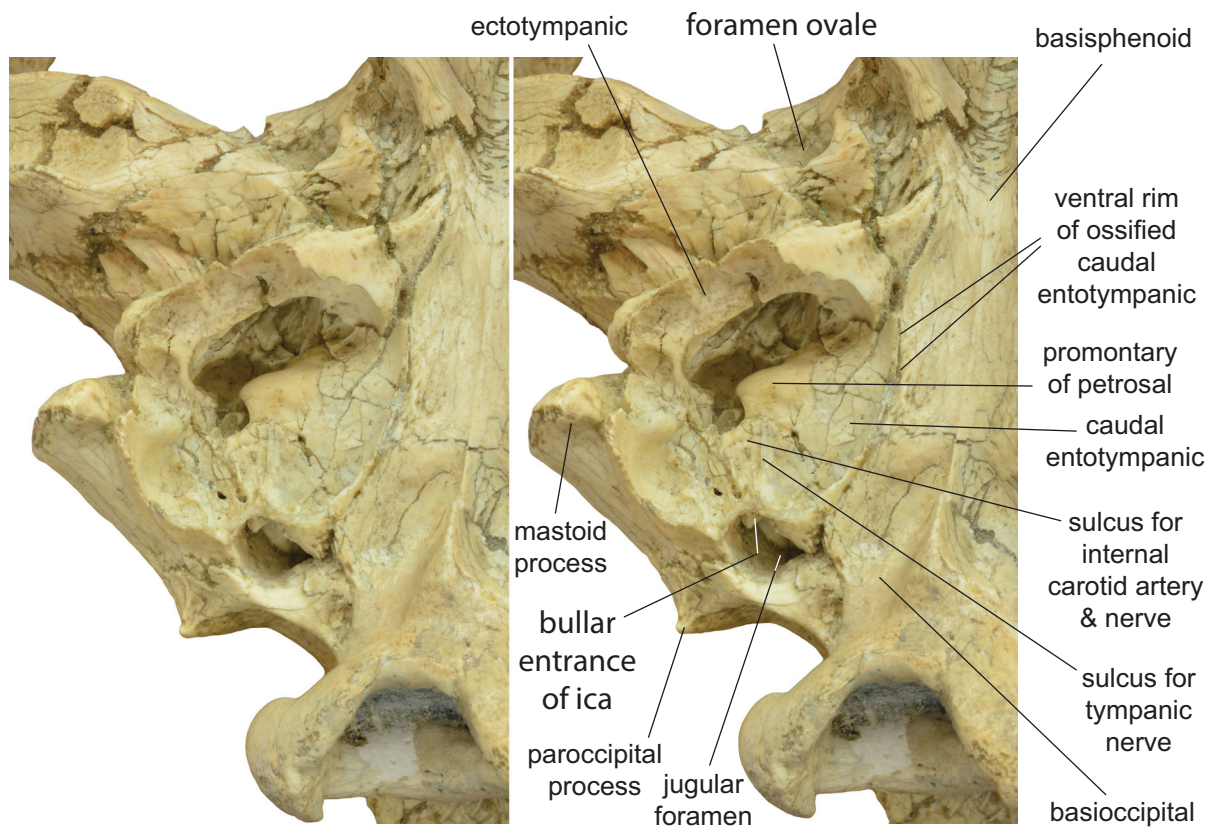


Figure 6. Stereophotographs of the right basicranium region of *Oriensmilus liupanensis* (IVPP V25220) in ventral view (top is anterior).

The left and right bullae of IVPP V25220 are partially preserved. The ventral floors are missing. Ventral edges of the right bulla are sharp and have the appearance of a tapering edge. These tapering edges seem to indicate a lack of ossification along the rim instead of non-preservation of bones, as is common in nimravines (Neff 1983; Hunt 1987), and the rest of the bullae were presumably cartilaginous. A good example of an ossified ventral edge of the bullae in presumed contact with cartilaginous bullar floors is seen in the holotype of *Dinictis cyclops* (AMNH 6937) (Fig. 8), a condition mentioned in Neff's (1983) dissertation.

The dorsal edge of the caudal entotympanic is in contact with the petrosal, surrounding the promontory of the petrosal. Although not visible in the dissected ventral view, a small, thin, oval-shaped rostral entotympanic can be discerned in CT images (Fig. 9). This bone is exactly at the position where Hunt (1987, fig. 5) first

documented a small rostral entotympanic bone in a juvenile specimen of *Dinictis* (UNSM 4051-81). Along the medial side of the bulla, there is no sign of a ventral process of the petrosal, as observed by Hunt (1989) in all living feliforms except Felidae (but present in the basal felid *Proailurus*).

The most striking feature of the bullar region is the presence of a small foramen on the posterior wall of the caudal entotympanic just below the large confluence of the jugular foramen. This foramen is fully preserved on the right side of IVPP V25220, whereas on its left side the ventral half of the enclosure is missing. In the holotype of *Dinictis cyclops*, this foramen is also well preserved as indicated by a smooth surface of arterial impression across the exposed bullar wall, although its (presumed cartilaginous) ventral enclosure is missing (Fig. 8). The posterior bullar wall forms a small septum-like structure projecting toward the inside of the

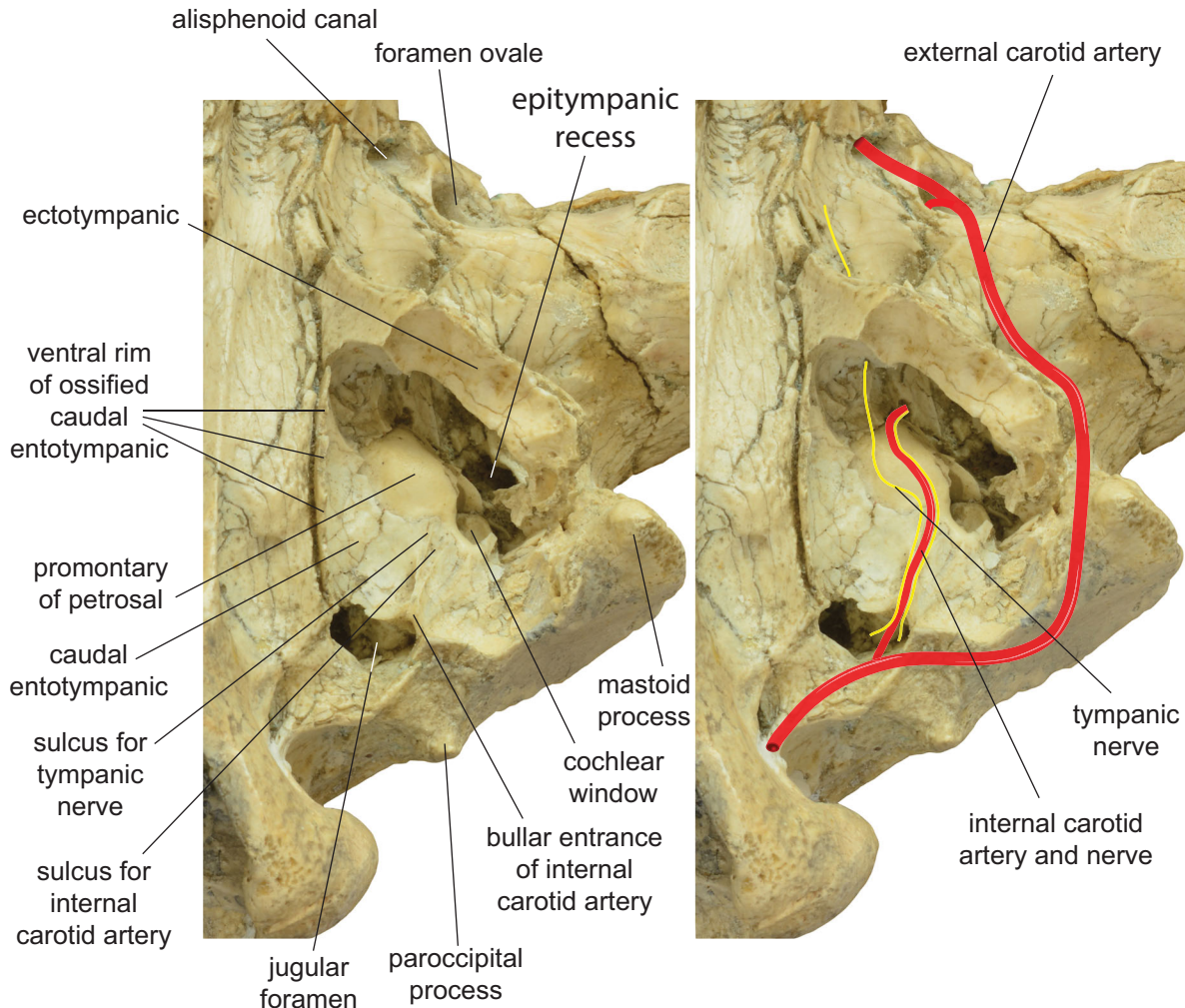


Figure 7. Stereophotographs of the left basicranium region of *Oriensmilus liupanensis* (IVPP V25220), with reconstruction of the arteries (red) and nerves (yellow) in ventral view (top is anterior).

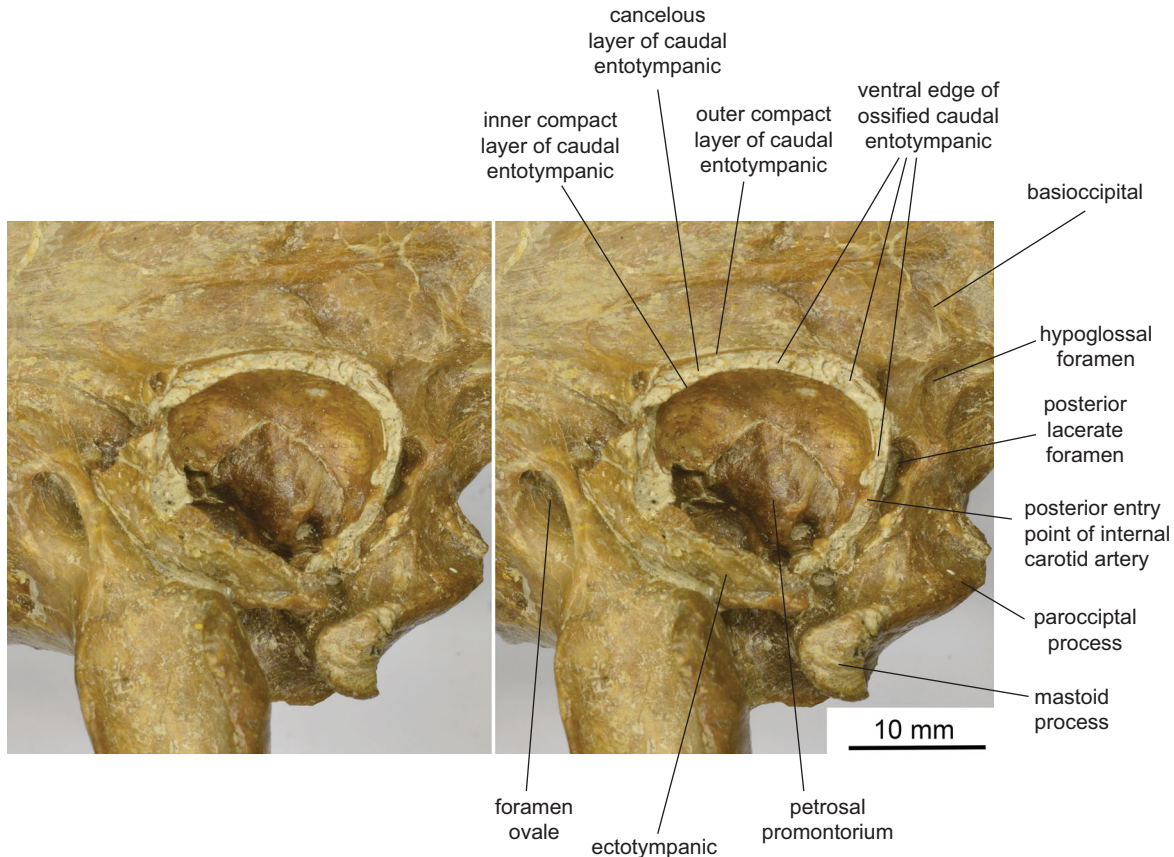


Figure 8. Bullar structure of *Dinictis cyclops* (AMNH 6937, holotype), first described by Neff (1983). The unossified ventral portion of the caudal entotympanic and posteroventral entry of the internal carotid artery are two primitive characters still preserved in *Oriensmilus liupanensis*.

bullar space. On either side of this septum (on the right bulla) or along its crest (on the left bulla) are distinct longitudinal grooves presumably left by the internal carotid artery and nerve and tympanic nerve (Figs 6, 7). The impressions left by blood vessels and nerves are only preserved on the caudal entotympanic surface, but not on the smooth-surfaced petrosal promontorium. In earlier nimravids, promontorial grooves are also observed, as in the *Dinictis* sp. skull (F:AM 62034) illustrated by Neff (1983, figs 31, 32). In a specimen of *Hoplophoneus* sp. (AMNH 82440) dissected by Neff (1983, figs 38, 39), this posterior entry of the carotid artery from behind the petrosal promontory through a foramen in the bullar wall is also illustrated, in the same position as the Tongxin *Oriensmilus*. Similarly, the ventral edge of the ectotympanic is also tapered, appearing to form a natural contact of the unossified bullar floor. As far as we are aware, this unique posterior entry and transpromontorial position of the internal carotid artery, as reconstructed in Figures 7 and 9, is unique in Nimravidae.

Taxonomic remarks on Chinese barbourofelines

Chinese records of barbourofelines are limited but growing. ‘*Sansanosmilus palmidens*’ (here referred to *Oriensmilus liupanensis*) was first reported from the early part of the middle Miocene (early Tunggurian) locality of Jiulongkou, Cixian County, Hebei Province in northern China (Chen & Wu 1976). A larger species (AMNH 26608), here tentatively assigned to *Albanosmilus jourdani*, was documented in the later part of the middle Miocene (late Tunggurian) locality of *Platybelodon* Quarry and at the stratigraphically lower Tairum Nor localities in the Tunggur Formation (Colbert 1939; Qiu *et al.* 1988a, 2013; Wang *et al.* 2003) (Fig. 1).

We include the Jiulongkou materials from Hebei Province (Chen & Wu 1976) in *Oriensmilus liupanensis* because of their comparable dental dimensions to those from Tongxin (Table 1) and the presence of a distinct P4 protocone. We note, however, that the posterior accessory cusp of the P3 in the Jiulongkou specimens is divided by a notch, a character seen in the type series of *Sansanosmilus palmidens*. Qiu *et al.* (2013b, fig. 14)

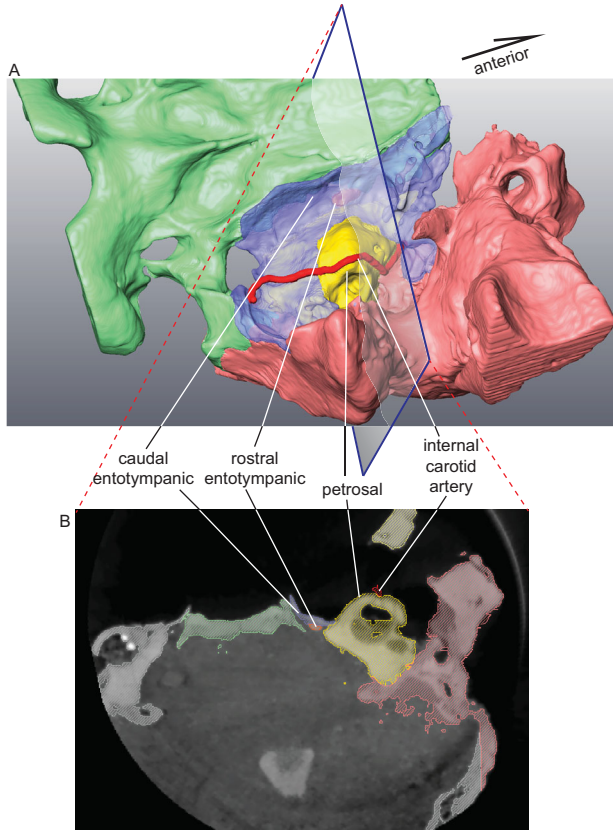


Figure 9. Segmentations of a CT-scan of the basicranial region of *Oriensmilus liupanensis* (IVPP V25220). **A**, ventral view of segmented elements including basioccipital and basisphenoid (green), caudal entotympanic (semi-transparent blue to reveal rostral entotympanic underneath), petrosal (yellow), reconstructed internal carotid artery (red), and mastoid-glenoid region (pink). **B**, transverse cross-section (dark blue rectangle in A) of segmentation view in Avizo showing the labelled structures discussed in the text.

placed the Jiulongkou Fauna in the beginning of the Shanwangian Chinese Land Mammal age. If this is correct, the age range of *O. liupanensis* is extended into the early Miocene.

We also present a series of upper carnassials of barbourofelines from several Chinese localities (Fig. 2) that permit a sense of dental evolution in eastern Asia, which largely mirrors that in Europe. In addition to the new Tongxin specimen (Fig. 2A–C), we include three isolated P4s from at least two stratigraphic horizons in the Tunggur Formation, Inner Mongolia (Fig. 2D–K). Increasing size and a decrease (and eventual loss) of the P4 protocone are readily discernible, although we do not currently understand the full variation in this character. We recognize two Chinese species, a number that might increase as more and better material becomes available.

With the primitive *Prosansosmilus* and terminal species *Barbourofelis fricki* on either ends of the

barbourofeline lineage, there is enough morphological and geographical continuity to observe trends in barbourofeline size increase and development of the hypercarnivorous dentition. The following interrelated characters are readily discernible in progressively more advanced barbourofelines: ventral expansion of mastoid process and glenoid fossa; expansion of ventral fossette of the mastoid process; more erect supraoccipital; formation of postorbital bar; enlargement of infraorbital foramen; shortening and broadening of palate; rotation of P3 and flaring of lower cheek teeth; ventral expansion of mandibular symphysis and flange; lengthening of carnassials; reduction and loss of P4 protocone; and recumbent cheek teeth. Using these polarized characters, one can derive a sense of the stage of evolution among different forms.

The Gunziling specimen falls toward the primitive end of the spectrum. Overall, it is comparable in size and cranial proportions to *Sansanosmilus palmidens* from Sansan (Blainville 1841; Ginsburg 1961; Peigné 2012) (Table 1). However, it has the following mostly primitive characters that distinguish it as a more primitive species: ventral floor of bulla not ossified; medial bullar walls not expanded toward each other (bulla less inflated); less downwardly expanded occipital condyle; more rounded profile for supraoccipital shield; more posteriorly tapered pterygoid; less enlarged postorbital process of frontal and a postorbital bar being absent; somewhat broadened palate with a more inwardly rotated P3; P3 lacking a notch on the posterior accessory cusp, which helps to delineate an extra posterior cusp in *S. palmidens*; lingually swollen P3 but no distinct cusp or root associated with this swelling; presence of a small protocone on P4, which is absent in *S. palmidens*; and less reduced M1.

Notably, the complete lack of an ossified ventral bullar floor from our Tongxin specimen is in sharp contrast to the fully ossified bulla from Sansan (Blainville 1841; Ginsburg 1961). The latter's advanced stage of bullar ossification is comparable to those in North American *Barbourofelis* (Baskin 1981). Assuming a linear progression of ossification, our Chinese specimen helps to delineate the time of the transition of this character among Eurasian forms.

Besides its smaller size, AMNH FM 145755 is also primitive in the following characters: lack of postorbital bar; small infraorbital canal; small and low crowned P4 preparastyle; a small P4 protocone; relatively high and unreduced coronoid process; double rooted p3; p4–m1 cusps not recumbent; deep notches between accessory cusps and main cusp of p4; and deep carnassial notch. These characters are consistent with those on IVPP

V25220 and make a good case that the two Tongxin specimens belong to the same species.

To allow for a sense of stage of evolution relative to primitive North American and derived Eurasian forms, the skull fragment (F:AM 69453) of *Barbourofelis whitfordi* from MacAdams Quarry was used for comparison. Two characters clearly show that *B. whitfordi* is more derived than IVPP V25220: a significantly enlarged infraorbital canal and a more strongly reduced P3 relative to P4. An estimated ratio of P3/P4 length of 0.29 (9.2/32.0 mm) for F:AM 69453 contrasts with that of IVPP V25220 (0.49: 14.0/28.8 mm). Conversely, the P4 in AMNH 26608 (length 37.0 mm) from the upper part of the Tunggur Formation (Colbert 1939, fig. 19; Wang *et al.* 2003) (Fig. 2J, K) is much longer than that of F:AM 69453 (32.0 mm; measurements based on dimensions of roots), and falls in the lower range of *B. morrisoni* (35.8–45.1 mm) and nearly reaches the size of *Albanosmilus/Barbourofelis piveteaui* (40.3 mm). Furthermore, the anterior root of the P4 in F:AM 69453 shows a lingual bulge that indicates the presence of a small remnant of a protocone (the P4 is estimated to be approximately 10 mm in width including this bulge), probably equivalent to the condition seen in the single P4, IVPP V25221 (Fig. 2D–F), collected from the Tairum Nor locality of Tunggur Tableland (lower part of Tunggur Formation). This latter specimen, however, is slightly more advanced in its smaller P4 protocone than that from Tongxin. Although suffering from extensive wear, the enamel where the protocone should be (immediately ventral to a faint bulge on the anterior root of AMNH 26608) is still preserved and shows no indication of a protocone (Fig. 2J, K), reaching the condition seen in all individuals of *B. morrisoni*.

The cranial morphology of the Tongxin specimens also has a number of primitive features. In the IVPP Tongxin specimen, the posterior suture of the nasal ends just anterior to the orbit, whereas that in *Barbourofelis morrisoni* is posteriorly expanded to reach beyond the orbit. The top of the frontal is flat with a slight hint of a concavity, in contrast to a more prominent concavity in *B. morrisoni*. The dorsal profile of the skull is also very flat instead of being elevated toward the posterior half as in *Barbourofelis*. The infraorbital canal is much smaller than in *B. morrisoni*. The scar for the masseter muscle is also far less excavated, as in *B. morrisoni*. The temporal crests are rather vague, in contrast to the more sharply defined crest in *B. morrisoni*, and the sagittal crest is low.

Barbourofeline phylogeny

We modified the most recent character matrix of Robles *et al.* (2013), which was an adaptation of Geraads &

Güleç (1997) plus Morlo *et al.* (2004) (Table 2). However, we note that Robles *et al.*'s (2013) matrix suffers from an uncritical acceptance of felids as basal to barbourufelines, i.e. failing to take into account basicranial characters (see Family relationships, below). Additionally, Robles *et al.*'s (2013) hypothetical ancestor approach to an outgroup is also questionable (Bryant 1997). Instead we use actual taxa for outgroups and select *Nandinia binotata* as an outgroup for living Feliformia (Hunt 1974; Wible & Spaulding 2013) and '*Miacis*' *sylvestris* (see Wang & Tedford 1994) as a generalized basal miacoid that may be more stem-ward for all living families of Carnivora (Spaulding & Flynn 2012). Lastly, we also added *Dinictis* to the matrix because of its well-known basicranial morphology (Hunt 1987).

Our modified data matrix is provided as Supplemental material. A total of 11 trees were found using the Implicit Enumeration search option and Figure 10 shows a majority rule consensus tree (cut-off at 50) produced using TNT. Our tree shows that nimravines and barbourufelines are sister taxa to the exclusion of felids. Our phylogeny places *Dinictis* at the stem of the barbourufelines and this is likely an artefact of limited sampling for the other nimravines. Similarly, an apparent sister-group relationship between felids and nimravids is an artefact of excluding other feliform carnivorans from the analysis. Only complete coding for all feliforms could begin to tackle these questions.

Oriensmilus is a transitional form toward the more derived taxa and represents the first barbourufeline appearance in Asia that evolved from an apparent European *Prosansanosmilus* progenitor. The Chinese *Oriensmilus* existed in parallel with the European *Sansanosmilus* during the beginning of the middle Miocene. By the later middle Miocene, *Albanosmilus* replaced *Oriensmilus* in China and dispersed to North America to give rise to *Barbourofelis*. The status of '*Barbourofelis*' *piveteaui* is still unclear – additional material is needed to decide whether it represents an indigenous, highly derived form in central Turkey or a reverse immigrant from North America.

Family relationships of barbourufelines

Based largely on North American Eocene–Oligocene forms and recognizing their different configurations of cranial foramina, Cope (1880) introduced a new family Nimravidae to be distinguished from the true cats (Felidae) and also coined the term 'false' sabretooth for his nimravids. At that time, barbourufelines were still poorly known (the subfamily name could not be in

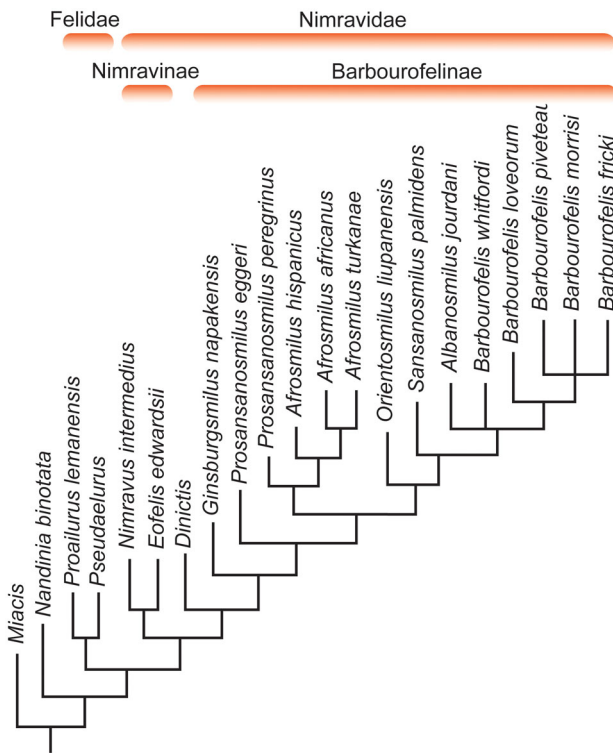


Figure 10. Majority rule consensus tree (cut-off at 50) from 11 equally parsimonious trees by implicit enumeration derived from a modified version of the data matrix of Robles *et al.* (2013) (see Supplemental material), as computed by TNT v. 1.5 (Goloboff & Catalano 2016). Tree length = 103 steps.

strongly signals the lack of a close relationship between the barbourofelines and felids, as advocated by different authors (Neff 1983; Hunt 1987).

In recent decades, however, a steady trickle of transitional records began to fill the gaps between ancestral barbourofelines, leading to the proposition that the clade originated in the early Miocene of Africa (Morales *et al.* 2001). Although still poorly known from only fragmentary dental remains, enough continuity in dental morphology from African basal genera, such as *Ginsburgsmilus*, *Afrosmilus* and *Syrtosmilus*, through Eurasian transitional forms, such as *Prosansanosmilus*, *Sansanosmilus* and *Albanosmilus*, to their terminal genus *Barbourofelis*, was gained to enable a revised phylogenetic framework that traced barbourofelines to its African ancestors (Morlo *et al.* 2004; Morlo 2006; Robles *et al.* 2013). Interestingly, the African basal ‘barbourofelines’ exhibit a dental pattern reminiscent of basal felids from Europe. Morales *et al.* (2001) thus revived the previously abandoned notion that barbourofelines are, after all, a sister group of felids. This revival has the added benefit of sidestepping the previously perceived gap in the fossil record between the group’s first appearance in Miocene and its presumed divergence time in the Eocene (Peigné 2003; Morlo *et al.* 2004). Although

Morales *et al.* (2001) cautioned that additional studies of the cranium were needed, this European school of thought has influenced recent studies of cat relationships that have included barbourofelines in felid phylogenies (Piras *et al.* 2013; Cuff *et al.* 2015).

Despite the popularity of these recent studies, there remains a substantial morphological gap between the basicranial morphology of advanced barbourofelines and basal felids (Hunt 1987). Recent cladistic analyses by Morlo *et al.* (2004) and Robles *et al.* (2013) proposed explicit dental transformations but questions regarding the basicranium remain unaddressed. Morales *et al.* (2001, 101), however, acknowledged that “without doubt we need additional evidence regarding the cranial morphology of *Ginsburgsmilus*, *Afrosmilus*, and *Prosansanosmilus*, together with a restudy of *Sansanosmilus*; this information would be fundamental for understanding the divergence between Barbourofelinae and Felinae”. With the exquisite preservation of our new Chinese material, we are in a position to address these lingering challenges.

Baskin (1981, fig. 2) illustrated a fragmentary left ear region of *Barbourofelis loveorum* (UF 24432). Two features stand out in this specimen. First, a small rostral entotympanic bone was indicated in a similar position to that seen in *Oriensmilus* (Fig. 9). Second, a thin bony tube along the posterior bullar wall was identified as the posterior carotid foramen, which bears remarkable resemblance to the calibre, position and orientation of a similar groove (sulcus) for the internal carotid artery seen in *Oriensmilus* (Figs 6, 7). Although the elevated sulcus in *Oriensmilus* is not enclosed by bone, the two above-mentioned features provide strong evidence that a similar bullar composition and arterial configuration are shared by *Oriensmilus* and *Barbourofelis*. The elevated sulcus for the carotid artery in *Oriensmilus* makes an ideal transitional condition between the lack of this structure in *Dinictis* (Fig. 8) and the fully enclosed internal carotid tube in *Barbourofelis*.

Hunt (1989) identified a basicranium ‘bauplan’ for all families of feliforms (aeluroids) with a distinct ventral process of the petrosal promontory and a facet for the ectotympanic on the petrosal (impressions left by a full septum bulla), including the most basal feliform *Nandinia*, which falls outside of living families, plus other basal members of living families when they can be identified in the fossil record (Hunt 1991, 2001; Hunt & Solounias 1991). If the barbourofelines are truly a sister group to felids, to the exclusion of all other families of feliforms, then barbourofelines must have started off with a similar arrangement of the basicranium. Hunt (1987) was able to rule out *Dinictis* (i.e. nimravines) from this arrangement as well as advanced (North

American) species of *Barbourofelis*, which led him to place barbourofelines within Nimravidae.

Hunt (1987, figs 2, 3) also described a juvenile specimen of *Dinictis*, in which an ossified ventral edge of the caudal entotympanic along the medial side of the bulla is presumably in contact with a (unpreserved) cartilaginous ventral portion of the caudal entotympanic. He further observed that cancellous bones are sandwiched between the compact outer and inner layers of the entotympanic, a condition noted earlier by Neff (1983, fig. 28) in her unpublished dissertation but not seen in barbourofelines (Fig. 8).

Based on Baskin's (1981) initial description of the *Barbourofelis* ear region and Hunt's (1987) thorough description of the basicranium of *Dinictis*, plus the unpublished dissertation by Neff (1983), we can identify at least four shared characters between nimravines and barbourofelines: posterior entrance of the internal carotid artery/nerve; lack of an ossified bullar floor (in primitive barbourofelines); presence of a small rostral entotympanic dorsal to caudal entotympanic; and possibly the presence of a proseptum. Although the lack of a bullar ossification by itself is surely a primitive character, the way the presumed cartilaginous ventral floor attaches itself to the bulla rim is quite unique among carnivorans and shared by barbourofelines and nimravines only. In a poorly preserved auditory region of *Sansanosmilus* from Sansan (MNHN Sa3384), Morlo *et al.* (2004, fig. 6D) confirmed the presence of a proseptum (re-figured in Peigné 2012, fig. 150). In addition, ontogenetically, bulla formation is also different between *Dinictis* and living feliforms (Hunt 1987). If the preserved basicranial characters are any indication, barbourofeline bullar ontogeny is likely to be different as well. Furthermore, the postcranial skeleton of *Barbourofelis* is not felid-like and resembles nimravines in a number of structures, such as an atlas that lacks an alar notch (Baskin 2005), but it does converge with *Smilodon*.

The above-mentioned basicranial configurations of nimravines and barbourofelines are in stark contrast to those of felids. The middle ear region in modern felids is characterized by the presence of a complete intrabullar septum dividing the bullar space into two chambers (Hunt 1974). Furthermore, all feliforms possess a ventral promontorial process of the petrosal, although living felids have suppressed it by encroachment of an inflated auditory bulla (basal proailurine felids retain this process) (Hunt 1989), a character absent in nimravines and barbourofelines. The internal carotid artery and nerve enter the bulla via posterior lacerate foramen and lack a transpromontorial branch (Davis & Story 1943).

Based on new information from Chinese *Oriensmilus* and *Albanosmilus*, the barbourofelines are emphatically different from felid configurations in both basicranial morphology

and dental patterns. While the higher-level relationships with Nimravidae are yet to be settled (e.g. Neff 1983; Hunt 1987; Flynn *et al.* 2010), the inclusion of barbourofelines within nimravids is still the most viable option.

Conclusions

1. A nearly complete skull of *Oriensmilus liupanensis* gen. et sp. nov., a primitive form of Barbourofelinae sabretooth from the middle Miocene Tongxin Basin of northern China, has a well-preserved basicranial region that offers the opportunity to re-examine fundamental relationships between felids and nimravids.
2. *Oriensmilus* is a Chinese middle Miocene form that is more primitive than the contemporaneous European *Sansanosmilus*, suggesting a certain amount of biogeographical differentiation between eastern and western Eurasia. By the later part of the middle Miocene, Chinese *Oriensmilus* was replaced by *Albanosmilus*, which probably gave rise to North American *Barbourofelis*.
3. The skull of *Oriensmilus* has the following characteristics shared with nimravines: absence of an ossified entotympanic floor; absence of an intrabullar septum to divide the bullar space into two chambers; lack of a ventral promontorial process of the petrosal; presence of a small, oval-shaped rostral entotympanic on the dorsal side of the caudal entotympanic; and a caudal entrance of the internal carotid artery and nerve that pierces the caudal entotympanic bullar wall.
4. The lack of an ossified bullar floor in the Tongxin skull and its presence in those from the middle Miocene of Sansan, France, help to bracket the transition of the bullar ossification within a short interval in the early part of the middle Miocene.
5. The above-described spatial relationships in the bullar construction and the carotid artery configuration in the middle ear of *Oriensmilus* suggest a relationship to the nimravines. Previously recognized dental similarities to felids are likely due to convergence.

Acknowledgements

We wish to thank Dr Sotirios Tetradis for providing access to the NewTom 5G cone-beam CT scanner at the UCLA School of Dentistry, Section of Oral and Maxillofacial Radiology. We thank John Babiarz for providing casts of several key taxa from North America.

We greatly benefited from discussions with Qiu Zhanxiang regarding taxonomic treatments. We thank Carl Mehling of the American Museum of Natural History for providing the catalogue numbers of specimens in his care. Lars Werdelin and three other anonymous reviewers made very helpful suggestions to improve the manuscript. We are grateful to the Associate Editor, Pip Brewer, who has made extensive corrections to the English grammar as well as suggestions with phrasing. We appreciate the stewardship of the Editor, Paul Barrett, throughout the review process. We are indebted to field teams in Inner Mongolia during the past two decades that resulted in the slow but steady accumulation of new specimens from the Tunggur Formation.

Supplemental material

Supplemental material for this article can be accessed here: <https://doi.org/10.1080/14772019.2019.1691066>.

ORCID

Xiaoming Wang  <http://orcid.org/0000-0003-1610-3840>

References

- Averianov, A., Obratsova, E., Danilov, I., Skutschas, P. & Jin, J. 2016. First nimravid skull from Asia. *Scientific Reports*, **6**, 25812. doi:10.1038/srep25812
- Baskin, J. A. 1981. *Barbourofelis* (Nimravidae) and *Nimravides* (Felidae), with a description of two new species from the late Miocene of Florida. *Journal of Mammalogy*, **62**, 122–139. doi:10.2307/1380483
- Baskin, J. A. 2005. Carnivora from the late Miocene Love Bone Bed of Florida. *Bulletin of the Florida Museum of Natural History*, **45**, 413–434.
- Blainville, H. M. D. d. 1841. *Ostéographie ou description iconographique comparée du squelette et du système dentaire des cinq classes d'animaux vertébrés récent et fossiles pour servir de base à la zoologie et à la géologie. Carnassiers*. Arthus Bertrand, Paris, 976 pp.
- Bowdich, T. E. 1821. *An analysis of the natural classifications of Mammalia, for the use of students and travellers*. J. Smith, Paris, 115 pp.
- Bryant, H. N. 1988. Delayed eruption of the deciduous upper canine in the sabertoothed carnivore *Barbourofelis lovei* (Carnivora, Nimravidae). *Journal of Vertebrate Paleontology*, **8**, 295–306. doi:10.1080/02724634.1988.10011712
- Bryant, H. N. 1991. Phylogenetic relationships and systematics of the Nimravidae (Carnivora). *Journal of Mammalogy*, **72**, 56–78. doi:10.2307/1381980
- Bryant, H. N. 1996. 22. Nimravidae. Pp. 453–475 in D. R. Prothero & R. J. Emry (eds) *The terrestrial Eocene–Oligocene transition in North America, Part I: the chronostratigraphy of the Uintan through Arikarean*. Cambridge University Press, Cambridge.
- Bryant, H. N. 1997. Hypothetical ancestors and rooting in cladistic analysis. *Cladistics*, **13**, 337–348. doi:10.1006/clad.1997.0048
- Bryant, H. N. & Russell, A. P. 1995. Carnassial functioning in nimravid and felid sabertooths: theoretical basis and robustness of inferences. Pp. 116–135 in J. J. Thomason (ed.) *Functional morphology in vertebrate paleontology*. Cambridge University Press, Cambridge.
- Chen, G.-F. 1977. A new genus of Iranotheriinae of Ningxia. *Vertebrata Palasiatica*, **15**, 143–147.
- Chen, G.-D. 1978. Some mastodonts from Miocene of Ningxia. *Vertebrata Palasiatica*, **16**, 103–110.
- Chen, G.-D. & Wu, W.-Y. 1976. Miocene mammals from Jiulongkou, Cixian, Hebei Province. *Vertebrata Palasiatica*, **14**, 6–15.
- Chow, M.-C. 1958. A record of the earliest sabre-toothed cats of the Eocene of Lushih, Honan. *Science Record (New Series)*, **2**, 347–349.
- Colbert, E. H. 1939. Carnivora of the Tung Gur Formation of Mongolia. *Bulletin of the American Museum of Natural History*, **76**, 47–81.
- Cope, E. D. 1880. On the extinct cats of America. *American Naturalist*, **14**, 833–835. doi:10.1086/272672
- Cuff, A. R., Randau, M., Head, J. J., Hutchinson, J. R., Pierce, S. E. & Goswami, A. 2015. Big cat, small cat: reconstructing body size evolution in living and extinct Felidae. *Journal of Evolutionary Biology*, **28**, 1516–1525. doi:10.1111/jeb.12671
- Davis, D. D. & Story, H. E. 1943. The carotid circulation in the domestic cat. *Zoological Series of Field Museum of Natural History*, **28**, 5–47.
- Deng, T. 2003. New material of *Hispanotherium matritense* (Rhinocerotidae, Perissodatyloidea) from Laogou of Hezheng County (Gansu, China), with special reference to the Chinese Middle Miocene elasmotheres. *Geobios*, **36**, 141–150. doi:10.1016/S0016-6995(03)00003-2
- Ding, S.-Y., Zheng, J.-J., Zhang, Y.-P. & Tong, Y.-S. 1977. The age and characteristic of the Liuniu and the Dongjun faunas, Bose Basin of Guangxi. *Vertebrata Palasiatica*, **15**, 35–45.
- Flynn, J. J. & Galiano, H. 1982. Phylogeny of early Tertiary Carnivora, with a description of a new species of *Proictis* from the middle Eocene of northwestern Wyoming. *American Museum Novitates*, **2725**, 1–64.
- Flynn, J. J., Finarelli, J. A. & Spaulding, M. 2010. Phylogeny of the Carnivora and Carnivoramorpha, and the use of the fossil record to enhance understanding of evolutionary transformations. Pp. 25–63 in A. Goswami & A. Friscia (eds) *Carnivoran evolution: new views on phylogeny, form and function*. Cambridge University Press, Cambridge.
- Geraads, D. & Güleç, E. 1997. Relationships of *Barbourofelis piveteaui* (Ozansoy, 1965), a late Miocene nimravid (Carnivora, Mammalia) from central Turkey. *Journal of Vertebrate Paleontology*, **17**, 370–375. doi:10.1080/02724634.1997.10010981
- Ginsburg, L. 1961. La faune des carnivores Miocènes de Sansan (Gers). *Mémoires du Muséum National d'Histoire Naturelle, Série C, Geologie*, **9**, 1–187.

- Goloboff, P. A. & Catalano, S. A.** 2016. TNT version 1.5, including a full implementation of phylogenetic morphometrics. *Cladistics*, **32**, 221–238. doi:10.1111/cla.12160
- Google Earth Pro (Version 7.3.2.5487)** 2015. Available from Google Inc., Mountain View, CA.
- Guan, J.** 1988. The Miocene strata and mammals from Tongxin, Ningxia and Guanghe, Gansu. *Memoirs of the Beijing Natural History Museum*, **42**, 1–21.
- Guan, J. & Van der Made, J.** 1993. Fossil Suidae from Dingjiaergou near Tongxin, China. *Memoirs of the Beijing Natural History Museum*, **53**, 150–199.
- Guan, J. & Zhang, X.** 1993. The middle Miocene lithic and mammalian records from Ningxia and Lonzhong basins, northwestern China. *Memoirs of the Beijing Natural History Museum*, **53**, 208–236.
- Harrison, T., Delson, E. & Guan, J.** 1991. A new species of *Pliopithecus* from the middle Miocene of China and its implications for early catarrhine zoogeography. *Journal of Human Evolution*, **21**, 329–361. doi:10.1016/0047-2484(91)90112-9
- Hough, J. R.** 1952. Auditory region in North American fossil Felidae: its significance in phylogeny. *United States Geological Survey Professional Paper*, 243-G, 95–115.
- Hunt, R. M. Jr.** 1974. The auditory bulla in Carnivora: an anatomical basis for reappraisal of carnivore evolution. *Journal of Morphology*, **143**, 21–76. doi:10.1002/jmor.1051430103
- Hunt, R. M. Jr.** 1987. Evolution of the aeluroid Carnivora: significance of auditory structure in the nimravid cat *Dinictis*. *American Museum Novitates*, **2886**, 1–74. doi:10.1206/0003-0082(2001)330<0001:BAOTLL>2.0.CO;2
- Hunt, R. M. Jr.** 1989. Evolution of the aeluroid Carnivora: significance of the ventral promontorial process of the petrosal, and the origin of basicranial patterns in the living families. *American Museum Novitates*, **2930**, 1–32. doi:10.1206/0003-0082(2001)330<0001:BAOTLL>2.0.CO;2
- Hunt, R. M. Jr.** 1991. Evolution of the aeluroid Carnivora: viverrid affinities of the Miocene carnivoran *Herpestides*. *American Museum Novitates*, **3023**, 1–34.
- Hunt, R. M. Jr.** 2001. Basicranial anatomy of the living linsangs *Prionodon* and *Poiana* (Mammalia, Carnivora, Viverridae), with comments on the early evolution of aeluroid carnivorans. *American Museum Novitates*, **3330**, 1–24.
- Hunt, R. M. Jr. & Solounias, N.** 1991. Evolution of the aeluroid Carnivora: hyaenid affinities of the Miocene carnivoran *Tungurictis spocki* from Inner Mongolia. *American Museum Novitates*, **3030**, 1–25.
- Jiangzuo, Q.-G., Li, C., Wang, S. & Sun, D.** 2019. *Amphicyon zhanxiangi*, sp. nov., a new amphicyonid (Mammalia, Carnivora) from northern China. *Journal of Vertebrate Paleontology*, **38**, e1539857. doi:10.1080/02724634.2018.1539857
- Maddison, W. P. & Maddison, D. R.** 2018. Mesquite: a modular system for evolutionary analysis. Version 3.51. Updated at <http://www.mesquiteproject.org>, accessed 7 January 2019.
- Morales, J., Salesa, M. J., Pickford, M. & Soria, D.** 2001. A new tribe, new genus and two new species of Barbourfelinae (Felidae, Carnivora, Mammalia) from the early Miocene of East Africa and Spain. *Transactions of the Royal Society of Edinburgh: Earth Sciences*, **92**, 97–102.
- Morlo, M.** 2006. New remains of Barbourfelidae (Mammalia, Carnivora) from the Miocene of southern Germany: implications for the history of barbourfelid migrations. *Beiträge zur Paläontologie*, **30**, 339–346.
- Morlo, M., Peigné, S. & Nagel, D.** 2004. A new species of *Prosansanosmilus*: implications for the systematic relationships of the family Barbourfelidae new rank (Carnivora, Mammalia). *Zoological Journal of the Linnean Society*, **140**, 43–61.
- Neff, N. A.** 1983. *The basicranial anatomy of the Nimravidae (Mammalia: Carnivora): character analyses and phylogenetic inferences*. Unpublished PhD thesis, City University of New York, New York, 643 pp.
- Peigné, S.** 2001. A primitive nimravine skull from the Quercy fissures, France: implications for the origin and evolution of Nimravidae (Carnivora). *Zoological Journal of the Linnean Society*, **132**, 401–410.
- Peigné, S.** 2003. Systematic review of European Nimravinae (Mammalia, Carnivora, Nimravidae) and the phylogenetic relationships of Palaeogene Nimravidae. *Zoologica Scripta*, **32**, 199–229.
- Peigné, S.** 2012. Les Carnivora de Sansan. Pp. 559–660 in S. Peigné & S. Sen (eds) *Mammifères de Sansan*. Muséum national d'Histoire naturelle, Paris.
- Peigné, S. & Bonis, L. de.** 2003. Juvenile cranial anatomy of Nimravidae (Mammalia, Carnivora): biological and phylogenetic implications. *Zoological Journal of the Linnean Society*, **138**, 477–493.
- Peigné, S., Chaimanee, Y., Jaeger, J.-J., Suteethorn, V. & Ducrocq, S.** 2000. Eocene nimravid carnivorans from Thailand. *Journal of Vertebrate Paleontology*, **20**, 157–163.
- Piras, P., Maiorino, L., Teresi, L., Meloro, C., Lucci, F., Kotsakis, T. & Raia, P.** 2013. Bite of the cats: relationships between functional integration and mechanical performance as revealed by mandible geometry. *Systematic Biology*, **62**, 878–900. doi:10.1093/sysbio/syt053
- Piveteau, J.** 1931. Les chats des phosphorites du Quercy. *Annales de Paléontologie*, **20**, 107–163.
- Qiu, Z.-D., Wang, X. & Li, Q.** 2013. Chapter 5. Neogene faunal succession and biochronology of central Nei Mongol (Inner Mongolia). Pp. 155–186 in X. Wang, L. J. Flynn & M. Fortelius (eds) *Fossil mammals of Asia: Neogene biostratigraphy and chronology*. Columbia University Press, New York.
- Qiu, Z.-X. & Guan, J.** 1986. A lower molar of *Pliopithecus* from Tongxin, Ningxia Hui Autonomous Region. *Acta Anthropologica Sinica*, **5**, 201–207.
- Qiu, Z.-X., Yan, D.-F., Chen, G.-F. & Qiu, Z.-D.** 1988a. Preliminary report on the field work in 1986 at Tung-gur, Nei Mongol. *Chinese Science Bulletin (Kexue Tongbao)*, **33**, 399–404.
- Qiu, Z.-X., Ye, J. & Cao, J.-X.** 1988b. A new species of *Percrocuta* from Tongxin, Ningxia. *Vertebrata Palasiatica*, **26**, 116–127.
- Qiu, Z.-X., Ye, J. & Huo, F.-C.** 1988c. Description of a *Kubanochoerus* skull from Tongxin, Ningxia. *Vertebrata Palasiatica*, **26**, 1–19.
- Qiu, Z.-X., Qiu, Z.-D., Deng, T., Li, C.-K., Zhang, Z.-Q., Wang, B.-Y. & Wang, X.** 2013b. Chapter 1. Neogene land mammal stages/ages of China – toward the goal to establish an Asian land mammal stage/age scheme. Pp. 29–90 in X. Wang, L. J. Flynn & M. Fortelius (eds)

- Fossil mammals of Asia: Neogene biostratigraphy and chronology*. Columbia University Press, New York.
- Robles, J. M., Alba, D. M., Fortuny, J., De Esteban-Trivigno, S., Rotgers, C., Balaguer, J., Carmona, R., Galindo, J., Almécija, S., Bertó, J. V. & Moyà-Solà, S.** 2013. New craniodental remains of the barbouroufelid *Albanosmilus jourdani* (Filhol, 1883) from the Miocene of the Vallès-Penedès Basin (NE Iberian Peninsula) and the phylogeny of the Barbouroufelini. *Journal of Systematic Palaeontology*, **11**, 993–1022. doi:10.1080/14772019.2012.724090
- Schultz, C. B., Schultz, M. R. & Martin, L. D.** 1970. A new tribe of saber-toothed cats (Barbouroufelini) from the Pliocene of North America. *Bulletin of the University of Nebraska State Museum*, **9**, 1–31.
- Spaulding, M. & Flynn, J. J.** 2012. Phylogeny of the Carnivoramorpha: the impact of postcranial characters. *Journal of Systematic Palaeontology*, **10**, 653–677. doi:10.1080/14772019.2011.630681
- Steininger, F. F.** 1999. Chronostratigraphy, geochronology and biochronology of the Miocene “European Land Mammal Mega-Zone” (ELMMZ) and the Miocene “Mammal-Zones (MN-Zones)”. Pp. 9–24 in G. E. Rössner & K. Heissig (eds) *The Miocene land mammals of Europe*. Dr. Friedrich Pfeil, Munich.
- Tedford, R. H.** 1978. History of dogs and cats: a view from the fossil record. Pp. 1–10. *Nutrition and management of dogs and cats*. Ralston Purina Co., St. Louis.
- Teilhard de Chardin, P. & Leroy, P.** 1945. Les Félidés de Chine. *Publications de l’Institut de Géobiologie*, **11**, 1–58.
- Wang, S.-Q., Zong, L.-Y., Yang, Q., Sun, B.-Y., Li, Y., Shi, Q.-Q., Yang, X.-W., Ye, J. & Wu, W.-Y.** 2016. Biostratigraphic subdividing of the Neogene Dingjia’ergou mammalian fauna, Tongxin County, Ningxia Province, and its background for the uplift of the Tibetan Plateau. *Quaternary Sciences*, **36**, 789–809.
- Wang, X. & Tedford, R. H.** 1994. Basicranial anatomy and phylogeny of primitive canids and closely related miacids (Carnivora: Mammalia). *American Museum Novitates*, **3092**, 1–34.
- Wang, X., Qiu, Z.-D. & Opdyke, N. O.** 2003. Litho-, bio-, and magnetostratigraphy and paleoenvironment of Tunggur Formation (middle Miocene) in central Inner Mongolia, China. *American Museum Novitates*, **3411**, 1–31. doi:10.1206/0003-0082(2003)411<0001:LBAMAP>2.0.CO;2
- Wang, X., Xie, G.-P. & Dong, W.** 2009. A new species of crown-antlered deer *Stephanocemas* (Artiodactyla, Cervidae) from middle Miocene of Qaidam Basin, northern Tibetan Plateau, China, and a preliminary evaluation of its phylogeny. *Zoological Journal of the Linnean Society*, **156**, 680–695. doi:10.1111/j.1096-3642.2008.00491.x
- Werdelin, L. & Solounias, N.** 1991. The Hyaenidae: taxonomy, systematics and evolution. *Fossils and Strata*, **30**, 1–104.
- Wible, J. R. & Spaulding, M.** 2013. On the cranial osteology of the African palm civet, *Nandinia binotata* (Gray, 1830) (Mammalia, Carnivora, Feliformia). *Annals of Carnegie Museum*, **82**, 1–114. doi:10.2992/007.082.0101
- Ye, J., Qiu, Z.-X. & Chen, J.-Z.** 1989. Comparative study of a juvenile skull of *Platybelodon tongxinensis*. *Vertebrata Palasiatica*, **27**, 284–300.
- Ye, J., Qiu, Z.-X. & Zhang, G.-D.** 1992. *Bunolistriodon intermedius* (Suidae, Artiodactyla) from Tongxin, Ningxia. *Vertebrata Palasiatica*, **30**, 135–145.

Associate Editor: Pip Brewer